Radix Isatidis polysaccharide (*RIP*) resists the infection of QX-type infectious bronchitis virus via the MDA5/TLR3/IRF7 signaling pathway

Xuelian Xiang, Jiadai Lv, Mengyi Dong, Nianling Li, Yongxin Li, Andong Wang, Yuxi Shen, Shuyun Li, Jing Xu, Min Cui, Xinfeng Han, Jing Xia, and Yong Huang[1]

College of Veterinary Medicine, Sichuan Agricultural University, Huimin Road 211, Wenjiang, Chengdu, Sichuan 611130, China

ABSTRACT Although vaccines play a major role in the prevention of infectious bronchitis (**IB**), Anti-IB drugs still have great potential in poultry production. *Radix Isatidis polysaccharide* (**RIP**) is a crude extract of *Banlangen* with antioxidant, antibacterial, antiviral, and multiple immunomodulatory functions. The aim of this study was to explore the innate immune mechanisms responsible for RIP-mediated alleviation of infectious bronchitis virus (**IBV**)-induced kidney lesions in chickens. Specific-pathogen-free (**SPF**) chicken and chicken embryo kidney (**CEK**) cells cultures were pretreated with RIP and then infected with the QX-type IBV strain, Sczy3. Morbidity, mortality, and tissue mean lesion scores were calculated for IBV-infected chickens, and the viral loads, inflammatory factor gene mRNA expression levels, and innate immune pathway gene mRNA expression levels in infected chickens and CEK cell cultures were determined. The results show that RIP could alleviate IBV-induced kidney damage, decrease CEK cells susceptibility to IBV infection, and reduce viral loads. Additionally, RIP reduced the mRNA expression levels of the inflammatory factors IL-6, IL-8, and IL-1β by decreasing the mRNA expression level of NF-κB. Conversely, the expression levels of MDA5, TLR3, STING, Myd88, IRF7, and IFN-β were increased, indicating that RIP conferred resistance to QX-type IBV infection via the MDA5, TLR3, IRF7 signaling pathway. These results provide a reference for both further research into the antiviral mechanisms of RIP and the development of preventative and therapeutic drugs for IB.

Key words: Radix Isatidis polysaccharide, IBV, CEK cell, kidney, MDA5 signaling pathway

2023 Poultry Science 102:102534
https://doi.org/10.1016/j.psj.2023.102534

INTRODUCTION

Infectious bronchitis virus (**IBV**) belongs to the family *Coronaviridae*, the genus *Gammacoronavirus*, and has been classified into a number of different serotypes that cause acute and highly contagious disease in chickens, causing huge losses to the poultry industry (Kong et al., 2021; Zamzam et al., 2022; Zhang et al., 2022). Studies have shown that the main clinical signs of infectious bronchitis (**IB**) include coughing, sneezing, breathlessness, open-mouth breathing, rales, and depression, and that IBV can affect the respiratory tract, kidneys, oviducts, ovaries, heart, liver, and bursa of chickens (Ganapathy, 2021; Al-Rasheed et al., 2022; Gallardo et al., 2022). Due to incomplete proofreading mechanism of the coronavirus' RNA polymerase and gene recombination during genome replication, new variants or recombinant IBV strains are constantly emerging, complicating the development of appropriate control programs. The search for drugs capable of preventing or treating IBV has therefore become a research priority.

Banlangen is the dried root of *Isatis indigotica Fort*, a plant of the cruciferous family. It is used in traditional medicine for its heat-clearing and blood detoxification properties, and is used to treat fever of external origin, incipient warmth, sore throat, warm spots, mumps, dampness, carbuncles, and sores (Wang et al., 2021). *Radix Isatidis polysaccharide* (**RIP**), extracted from *Banlangen*, is an active protein polysaccharide with multiple physiological functions such as antioxidant, antibacterial, antiviral, and various immunomodulatory functions (Zhou and Zhang, 2013), and its non-toxic and residue-free characteristics are increasingly becoming the focus of medical research (Ni et al., 2009; Du et al.,

Received August 5, 2022.
Accepted January 19, 2023.

[1]Corresponding author: hyong601@163.com

2013; Liu et al., 2017). Studies have shown that RIP can prevent hepatitis B virus infection of HepG2.2.15 cells by activating the JAK/STAT signaling pathway and inducing antiviral proteins, inhibiting the expression of SOCS1 and SOCS3, and promoting the production of IFN-α (Echeverría-Bugueño et al., 2021). In addition, RIP has been shown to significantly suppress the expressions of proinflammatory molecules, such as IL-6, IP-10, MIG, and CC chemokine motif ligand 5 (**CCL-5**) post H1N1 infection by inhibiting the TLR3 signaling pathway (Li et al., 2017). After LPS stimulation, RIP can also inhibit the production of reactive oxygen species (**ROS**), lipid peroxidation, nitric oxide (**NO**), prostaglandin E2 (**PGE2**), TNF-α, IL-6, and IL-8 in mouse alveolar macrophages (Shin et al., 2010). RIP has also been shown to enhance resistance to endotoxin and increase the expression levels of IL-2 and IFN-γ in immunocompromised mice as well as improve hemolysin levels and enhance the phagocytic activity of macrophages to promote adaptive immune responses in mice (Li et al., 2007; Zhao et al., 2008). The abuse of antibiotics has become a major concern in animal husbandry, and it has become imperative to find safe and effective alternatives to antibiotics for use as feed additives that can enhance immunity to viral infections. However, few studies have investigated the molecular mechanistic effects of RIP in the prevention and treatment of coronavirus.

To explore the potential mechanisms exerted by RIP against IBV, chicken were infected with the QX-type IBV, which has been the most common IBV genotype in China in recent years. We selected the MDA5 and TLR3 signaling pathways, which are associated with antiviral immunity, to study the effects of RIP on IBV infection. Morbidity and tissue mean lesion scores (**MLS**) of kidneys were calculated for infected chickens, and the viral loads and mRNA expression levels of inflammatory factor genes and antiviral signaling pathway genes in the kidneys of IBV infected chickens and CEK cells were determined. This study will provide a preliminary understanding of how RIP can be used against IBV infection and provides a reference for the future use of RIP in IB control.

MATERIALS AND METHODS

Virus, Medicines, and Chicken Embryos

The China/Sichuan/QX-like/Sczy3/200904 strain (Sczy3, GenBank JF732903, hereafter referred to as zy) was isolated from IBV infected broiler chickens (Sichuan, China) in 2009, and found to be a GI-19/QX-like IBV (Xia et al., 2018). The Traditional Chinese medicines RIP, Andro, and *Astragalus polysaccharides* (**APS**) were purchased from Yanglingciyuan Biotechnology company (Xi'an, China). Specific-pathogen-free (**SPF**) chicken embryos were obtained from Beijing Boehringer Ingelheim Vital Laboratory Animal Technology Co., Ltd. (Beijing, China) and were hatched in our lab. The zy strain was propagated in 10-day-old SPF chicken embryos and identified.

Quantitative Real-Time RT-PCR Validation (RT-qPCR)

Total RNA was extracted from the kidney with Trizol reagent (Thermo Fisher) and reverse-transcribed with the Reverse TranscRIPtion Kit (Takara, Japan). For the real-time RT-qPCR assays, specific primer pairs were designed to amplify the viral RNA of IBV, the mRNA of the inflammatory factors IL-6, IL-8, IL-1β, and NF-κB, the mRNA of the innate immune related genes MDA5, TLR3, STING, Myd88, IRF7, and IFN-β, as well as β-actin, using Primer Premier 5.0 software (Premier Biosoft International) (Table 1). The procedure for the quantification of viral load was performed as described previously (Li et al., 2022).

Animal Test

SPF chickens were randomly divided into eight groups, including control (n = 10 chicken), zy (n = 12), Andro (n = 12), APS (n = 12), RIP (n = 12), Andro + zy (n = 22), APS + zy (n = 22), and RIP + zy groups (n = 22), and kept in a negative pressure isolator. Chicken were held in separate biosafety level 2 (**BSL2**) isolators with ad libitum access to food and water and maintained under uniform standard conditions.

The Andro and Andro + zy groups were treated with Andro at a dose of 20 mg/kg/d; the RIP and RIP + zy groups were treated with RIP at a dose of 20 mg/kg/d; the APS and APS+zy groups were treated with APS at a dose of 20 mg/kg/d at 11 to 18 days of age. All treatments were administered orally. At the same time, the control and zy groups received the same volume of ddH_2O. At 19 d of age, the zy, Andro + zy, APS + zy,

Table 1. Primer sequences for qPCR.

cDNA	Primer sequences	cDNA	Primer sequences
IL-6-F	TCCCTCCTCG CCAATCT	TLR3-F	GCAACACTTCATTG AATAGCCTTGAT
IL-6-R	GGCCCTCACG GTCTTCT	TLR3-R	GCCAAACA-GATTTCC AATTGCATGT
IL-1β-F	AACCCGACC AGGTCAACA	STING-R	CGTGGCAGA ACTACTTTCAG
IL-1β-R	CGGTACATAC GAGATGGAAA	STING-F	TGACCGAGAGC TCCAAGAAG
IL-8-F	CACTTATGGCC AAGGCTCAG	Myd88-F	TGGAGAACTCA-TAG AAAGAAGG
IL-8-R2	ACCGATGTGGA AGGTGGAAG	Myd88-R	TGGGGAAAGAC TAAGAGCAAAT
IFN-β-F	TTCTCCTGCA ACCATCTTC	NF-κB-F	CGACCTGGATGTC AGGGACT
IFN-β-R	GAGGTGGAG CCGTATTCT	NF-κB-R	TGGAGACATGTA TGGCCGTT
MDA5-F	TAAGTGGAAATA CAGGAGGA	IRF7-F	AAGCCCAAGGA GTCCAAGC
MDA5-R	TCTTTCCAACAG ATGTTTCCA	IRF7-R	GCTGACGTTGCC ACTGTTGA
β-actin-F	CTGACTGACCG CGTTACTCC	β-actin-R	CATACCAACCAT CACACCCT

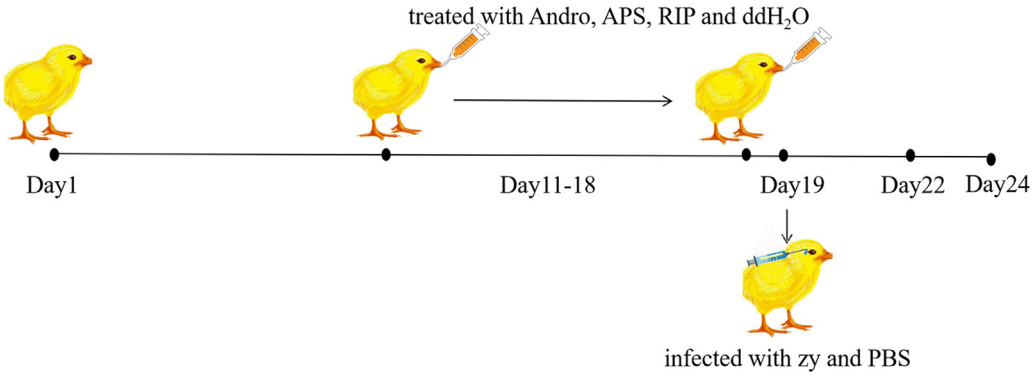

Figure 1. Schematic diagram of the experimental design. Note: The Andro and Andro + zy groups were treated with Andro at a dose of 20 mg/kg/d; the RIP and RIP + zy groups were treated with RIP at a dose of 20 mg/kg/d; the APS and APS + zy groups were treated with APS at a dose of 20 mg/kg/d at 11 to 18 d of age. All treatments were administered orally. The control and zy groups received the same volume of ddH_2O. At 19 d of age, the zy, Andro + zy, APS + zy, and RIP + zy groups were infected with zy at a dose of 10^5 EID_{50} per chicken in 0.2 mL via the intraocular and intranasal routes. The control, Andro, APS, and RIP groups received 0.2 mL of sterilized PBS.

and RIP + zy groups were each infected with zy at a dose of 10^5 EID_{50} per chicken in 0.2 mL via the intraocular and intranasal routes (Figure 1). The control, Andro, APS and RIP groups received 0.2 mL of sterilized PBS. Clinical signs were observed for 3 d and the morbidity determined. At 3 and 5 d postinfection (dpi), 5 chickens in each group were randomly selected and euthanized, respectively. Then, the percentage of swollen kidneys with tubules and ureters distended with urates at 5 dpi were calculated. Moreover, mean lesion scores (**MLS**) for the kidneys at 3 and 5 dpi were calculated. The gross lesions of the kidneys were scored as follows: 0 points, normal; 1 point, kidney swelling; and 2 points, mottled kidney. The medicine that best suppressed clinical symptoms and alleviated renal lesion development following IB infection was used in the subsequent study. One kidney from each chicken was obtained and stored in liquid nitrogen for subsequent RT-qPCR analysis, while the other kidney was subjected to histopathological analysis. Kidneys with different lesion scores were collected and stored in 10% neutral formalin for 24 h, embedded in paraffin, and stained with hematoxylin and eosin (**HE**) before being observed under a standard light microscope. Quantification of viral load and the mRNA levels of the inflammatory factors and innate immune related genes were performed as described above.

Cell Infection Tests

CEK cells were prepared and cultured as previously described (Li et al., 2007). Primary CEK cells were prepared from the kidneys of 18 to 20-day-old SPF chicken embryos and cultured in 48-well cell culture plates with Dulbecco's Modified Eagle Medium (DMEM; Gibco, Grand Island, NY) supplemented with 10% fetal bovine serum (FBS; Zhejiang Tianhang Biological Technology Stock Co., Ltd., Zhejiang, China), penicillin (100 U/mL), and streptomycin (100 μg/mL). The zy strain was propagated in primary CEK cells cultured in DMEM supplemented with 2% FBS at 37°C under 5% CO_2.

The CEK cell cultures were divided into four groups (control, RIP, zy, RIP + zy) when the confluency reached 70 to 80%. The RIP and RIP + zy groups were incubated with 200 μg/mL RIP dissolved in DMEM containing 2% FBS and the other two groups were incubated with DMEM containing 2% FBS. After 24 h, the RIP was removed from the CEK cell cultures, and the zy group and RIP + zy group CEK cells were infected with 100 $TCID_{50}$ of zy strain and cultured in DMEM with 2% FBS, while the control and RIP groups were not infected. The CEK cells were collected at 12, 24, 36 h postinfection (hpi) and subjected to RT-qPCR analysis as described above.

Statistical Analysis

The data were analyzed using SPSS version 24 (Chicago, IL) and expressed as the means ± standard deviations (***SD***). All the qPCR assays were repeated in triplicate, and the relative expression levels were measured in terms of threshold cycle (Ct) values and normalized via the formula $2^{-\Delta\Delta Ct}$. Differences between groups were compared using one-way analysis of variance (ANOVA) followed by Tukey's honestly significant difference (**HSD**) test. Data were expressed as mean ± SD. The significant thresholds were; $P < 0.05$ was considered significant, $P < 0.01$ was considered highly significant, $P < 0.001$ was considered very highly significant, while $P < 0.0001$ was considered very highly significant.

RESULTS

Clinical Signs and Pathological Lesions

In the zy group, IB symptoms appeared 1 dpi and spread rapidly to the entire group, becoming significantly worse on 2 dpi. The chicken exhibited gasping, coughing, sneezing, tracheal rales, and nasal discharge symptoms. By 3 to 5 dpi, clinical signs such as depression, ruffled feathers, white droppings and increased water intake among infected chicken were obvious. Feed consumption and weight gain were significantly reduced. Morbidity

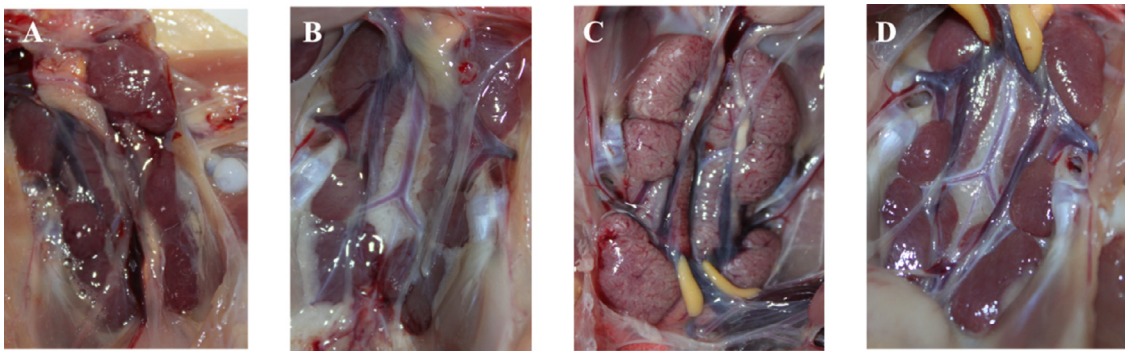

Figure 2. Renal swelling and swollen kidney with tubules and ureters distended with urates under different treatments. (A) Control; (B) RIP; (C) zy; and (D) RIP + zy.

rates for zy, Andro + zy, APS + zy, and RIP + zy groups were 83.3% (10/12), 63.6% (14/22), 59.1% (13/22), and 31.8% (7/22), respectively. At 5 dpi, kidneys from zy-infected chicken had swelled while the tubules and ureters were enlarged with urates (Figure 2). In the zy, Andro + zy, APS + zy, and RIP + zy groups, the percentages of swollen kidneys with tubules and ureters distended with urates were 60.0% (3/5), 0%, 20.0% (1/5), and 20.0% (1/5), respectively. Even though difference in MLS values between zy challenge group and RIP + zy group at 3 dpi was not significant, the RIP + IBV group had the lowest MLS value compared to the Andro + IBV and APS + IBV groups at 5 dpi (Figure 3).

The HE staining results showed that, in the zy infection group, vasodilatation, congestion, lymphocytic infiltration in kidneys, vacuolar degeneration, necrosis, and shedding of tubular epithelial cells, glomerular capsule dilation, necrosis and atrophy of glomeruli epithelial cells were observed. In the RIP + zy group, cell arrangement was neater and renal tubular epithelial cell structures were clearer, relative to the zy group. These findings imply that RIP significantly suppressed degeneration, necrosis, as well as atrophy of glomerular epithelial cells and lessened lymphocytic infiltration (Figure 4).

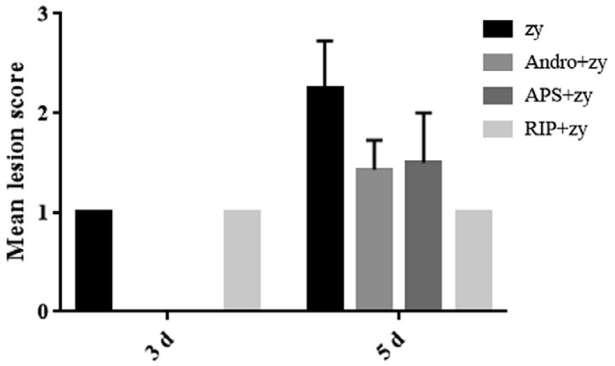

Figure 3. The mean lesion scores for the kidneys of the zy and RIP +zy groups at 3 and 5 dpi.

Viral Load Quantification in Kidneys of Chickens Infected by IBV zy Strain

We quantified the viral loads in the kidneys of the zy and RIP + zy groups. We found that the mean viral load in the kidneys of the RIP + zy group was significantly lower than that measured in the kidneys of the zy group at 3 dpi and 5 dpi. The mean viral load in the RIP + zy group was found to be 4 times lower than that of the zy group at 5 dpi (Figure 5). It was found that RIP reduced the viral load in zy-infected kidneys at 3 and 5 dpi.

RIP Suppressed the Expressions of Inflammatory Cytokines in the Kidneys of Chickens Infected with IBV zy Strain

We measured the relative mRNA expression levels of the major antiviral inflammatory factors IL-6, IL-1β, IL-8, and IFN-β in the kidneys of the chickens (Figure 6). The results showed that there were no

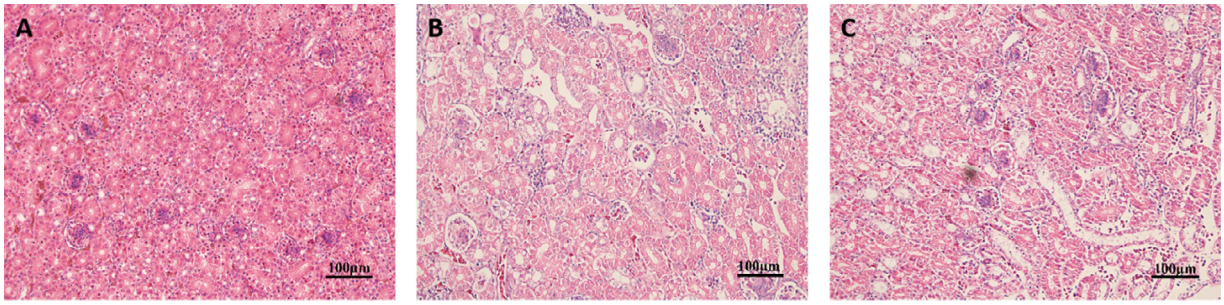

Figure 4. The effect of RIP on the histopathological changes (lesions) of chicken kidneys exposed to zy (200 × magnification). (A) Control; (B) zy; and (C) RIP+zy.

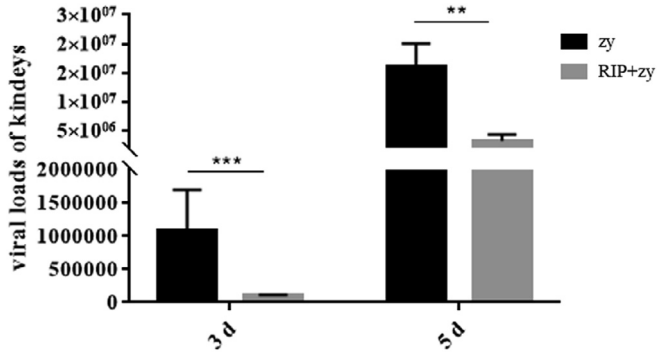

Figure 5. The viral loads in the kidneys of chickens in the zy and RIP + zy groups at 3 dpi and 5 dpi. Data are expressed as the means ± SD, n = 5. $^{*}P < 0.05$, $^{**}P < 0.01$, $^{***}P < 0.001$.

differences in the mRNA expression levels of IL-6, IL-1β, and IL-8 between the control group and the RIP group at 3 and 5 dpi. At 3 and 5 dpi, IL-6, and IL-1β expression levels were significantly upregulated in the zy group compared to the control group, whereas IL-8 expression levels were significantly upregulated at 5 dpi. Conversely, IFN-β expression levels were significantly downregulated in the zy group at 3 and 5 dpi compared to the control group. This demonstrates that IBV disrupts the homeostasis of the organism, causing a significant upregulation of proinflammatory factors and a decrease in the expression of antiviral interferon. Expressions of IL-6, IL-1β, and IL-8 were significantly downregulated in the RIP + zy group compared to the zy group at 5 dpi. IFN-β expression levels at 3 and 5 dpi were significantly upregulated in the RIP + zy group, compared to the zy group. Thus, RIP alleviated the increase in inflammatory cytokines levels in zy-infected kidneys.

RIP Conferred Resistance to Infection of Chicken with IBV zy Strain via the MDA5/TLR3/IRF7 Signaling Pathways

We measured the mRNA expression levels of the genes involved in the MDA5 and TLR3 signaling pathways (Figure 7). It was found that TLR3, STING, MyD88, and NF-κB expression levels did not differ significantly between the control and RIP groups at 3 and 5 dpi. MDA5 and IRF7 expression levels were significantly increased in the zy group compared to the control group at 3 and 5 dpi, whereas STING expression levels were significantly upregulated at 5 dpi. No significant difference in Myd88 expression levels was found between the zy group and the control group at 3 dpi but they were significantly downregulated at 5 dpi. The mRNA expression levels of NF-κB in the zy group showed significant downregulation at 3 dpi compared to the control group, but significant upregulation at 5 dpi. Compared to the zy group, mRNA expressions of MDA5, TLR3, STING, MyD88, and IRF7 in the RIP + zy group were significantly upregulated at 3 and 5 dpi. The mRNA expression levels of NF-κB were significantly downregulated in the RIP + zy group compared to the zy group at 5 dpi. These results show that RIP inhibited zy-infection of chicken via the MDA5/TLR3/IRF7 signaling pathways.

Principal Component Analysis

To observe the relationship between the mRNA expression levels of inflammatory factors, innate immune factors and the antiviral effect of RIP, a principal component analysis was performed. First, 3 principal components were extracted, each with an eigenvalue of greater than one and with 93.546% of the variance of the

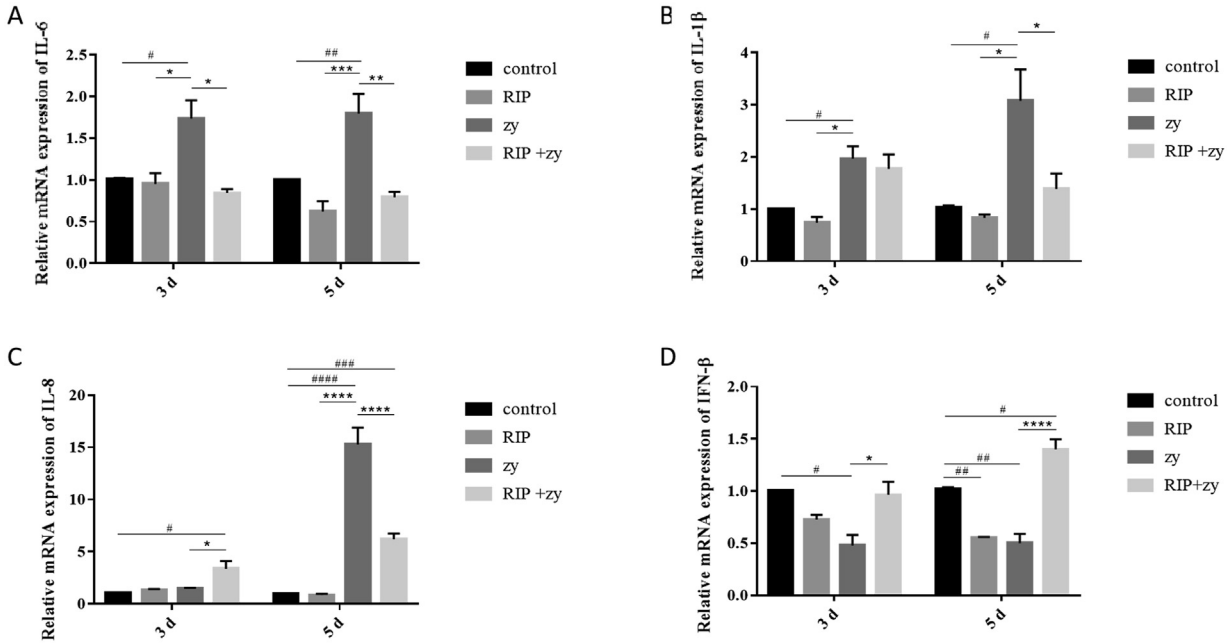

Figure 6. Effects of RIP on cytokines in chicken kidneys infected with zy. Relative mRNA expression levels of (A) IL-6, (B) IL-1β, (C) IL-8, and (D) IFN-β. Data are expressed as the means ± SD, n = 5. $^{\#}P < 0.05$, $^{\#\#}P < 0.01$, $^{\#\#\#}P < 0.001$, $^{\#\#\#\#}P < 0.0001$, compared to the control group; $^{*}P < 0.05$, $^{**}P < 0.01$, $^{***}P < 0.001$, $^{****}P < 0.0001$, compared to the zy group.

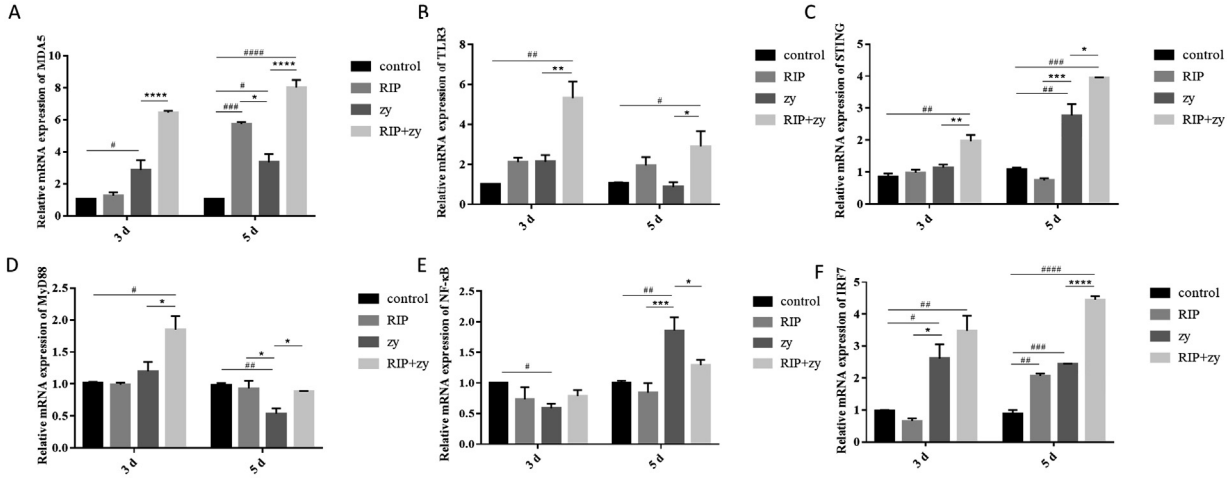

Figure 7. Effects of IPR on MDA5/TLR3 and downstream signaling pathways in the kidneys of chickens infected with zy. Relative mRNA expression levels of (A) MDA5, (B) TLR3, (C) STING, (D) Myd88, (E) NF-κB, and (F) IRF7. Data are expressed as the means ± SD, n = 5. $^{\#}P < 0.05$, $^{\#\#}P < 0.01$, $^{\#\#\#}P < 0.001$, $^{\#\#\#\#}P < 0.0001$, compared to the control group; $^{*}P < 0.05$, $^{**}P < 0.01$, $^{***}P < 0.001$, $^{****}P < 0.0001$, compared to the zy group.

Table 2. Principal components and extracted sums of variance for the chickens.

Component	Total	% of Variance	Cumulative %
1	6.544	65.444	65.444
2	1.589	15.887	81.332
3	1.221	12.215	93.546

3 principal components. Therefore the 3 principal components represent most of the variance of the results (Table 2).

Next, a rotated component matrix analysis was performed. The results showed that principal component 1 had a greater positive correlation with IL-8, MDA5, TLR3, STING, Myd88, and IRF7, and a greater negative correlation with NF-κB. Interestingly, principal component 2 had a greater positive correlation with IL-β, IFN-β, and TLR3, while principle component 3 had a greater positive correlation with IL-6 (Table 3).

Table 3. The rotated component matrix.

Indicators	Component 1	Component 2	Component 3
Relative mRNA expression of IL-6	−0.137	−0.092	0.973
Relative mRNA expression of IL-1β	0.497	0.841	0.095
Relative mRNA expression of IL-8	0.877	−0.068	−0.249
Relative mRNA expression of IFN-β	−0.033	0.871	−0.170
Relative mRNA expression of MDA5	0.895	0.413	−0.057
Relative mRNA expression of TLR3	0.668	0.710	−0.014
Relative mRNA expression of STING	0.898	0.360	−0.177
Relative mRNA expression of MyD88	0.835	0.464	0.258
Relative mRNA expression of NF-κB	-0.809	−0.031	−0.578
Relative mRNA expression of IRF7	0.750	0.604	0.055

The scores for each principal component were then calculated (Table 4). First, the scores for the inflammatory factors were calculated and the results showed that the RIP group and the zy group had a greater effect on principal component 1 and that these two groups showed an opposing state. It is worth noting that the zy group had a greater effect on principal component 3. Additionally, the scores for the control, RIP + zy, and RIP groups were similar, indicating that the influence of these two groups on the three principal components was similar, while the difference between the zy group and the other 3 groups was greater, indicating that the influence of zy on the 3 principal components was very different from the other three groups.

The scores for each of the three principal components were then used to calculate the group-specific scores for each principal component to calculate the scores for the innate immune factors (Table 5). The results showed that RIP + zy had a greater effect on principal component 1 and the control group had a greater effect on principal component 2. The control, RIP + zy, and RIP groups differed significantly from the zy group in their scores for the three principal components, demonstrating that the effect of zy on these 3 principal components differed significantly from the other 3 groups.

RIP Suppressed the Viral Load in CEKs after Infection of IBV zy Strain

To confirm that RIP can inhibit zy proliferation in CEK cells, we quantified the viral loads in the zy and RIP + zy groups at 12, 24, and 36 hpi (Figure 8). The RIP + zy group exhibited a significant decreasing trend when compared to the zy group at 24 and 36 hpi. These results imply that RIP suppressed the viral load in zy-infected CEKs at 24 and 36 hpi.

Table 4. Scores for the four chicken groups for the three inflammatory factor principal components.

Group	Component 1	Component 2	Component 3	Total	Bankin
Control	0.002329686	−0.047242835	−0.056655986	−0.101569135	4
RIP	0.489855036	−0.233999923	−0.213982664	0.041872448	2
zy	-0.787009462	0.17004884	0.684338753	0.06737813	1
RIP+zy	0.373432717	−0.105605499	−0.357759171	−0.089931953	3

Table 5. Scores for the four chicken groups for the four innate immune pathway gene principal components.

Group	Component 1	Component 2	Component 3	Total	Bankin
Control	−0.369132199	0.865	−0.086906822	0.408960979	2
RIP	−0.130260379	−0.448284608	0.118196837	−0.46034815	3
zy	−0.25320086	−0.491950364	0.100341776	−0.644809448	4
RIP+zy	0.644041209	0.275781946	−0.116720267	0.803102888	1

RIP Alleviated the Increase in Inflammatory Cytokine Levels in CEK Cells Infected with zy Strain

To investigate whether RIP can reduce inflammatory factors in vitro, we examined the mRNA expression levels of IL-6, IL-1β, IL-8, and IFN-β in CEK cell cultures at 12, 24, and 36 hpi (Figure 9). The results show that in the zy group, IL-6, IL-1β, and IL-8 levels were significantly increased at 24 and 36 hpi, compared to the control group. Compared to the zy group, IL-6, IL-1β, and IL-8 expressions were significantly decreased at 24 and 36 hpi in the RIP + zy group. At 12 and 24 hpi, the IFN-β expression levels significantly increased in the zy group compared to the control group, and compared to the zy group, the IFN-β expression levels significantly increased in the RIP + zy group. These results show that RIP alleviated the increase in inflammatory cytokines levels in CEK cells infected with zy strain.

RIP Conferred Resistance to Infection of CEK cells with zy Strain via the MDA5/TLR3/IRF7 Signaling Pathways

To investigate the expression of the signaling pathways induced by zy infection in CEK cells by RIP, we examined the mRNA expression levels of MDA5, TLR3, STING, MyD88, NF-κB, and IRF7 in CEK cell cultures at 12, 24, and 36 hpi (Figure 10). The results show that the mRNA expression levels of MDA5, TLR3, STING, MyD88, NF-κB, and IRF7 in the zy group were significantly increased at 24 and 36 hpi, compared to the control group. Expression levels of MDA5 in the RIP + zy group significantly increased at 24 hpi compared to the zy group, with no significant changes observed at the other time points. Compared to the zy group, expression levels of TLR3, STING, MyD88, and IRF7 were significantly elevated in the RIP + zy group at 12, 24, and 36 hpi. Compared to the zy group, NF-κB expressions in the RIP + zy group were significantly suppressed at 24 and 36 hpi. These results show that RIP inhibited zy infection of CEK cells via the MDA5/TLR3/IRF7 signaling Pathways

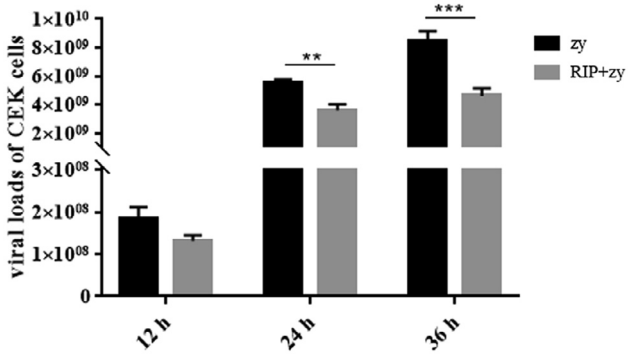

Figure 8. The mRNA expression of viral load in the zy and RIP + zy groups at 12 and 24 hpi. Data are expressed as the means ± SD, n = 5, $^{*}P < 0.05$, $^{**}P < 0.01$, $^{***}P < 0.001$.

DISCUSSION

IBV is an economically significant poultry disease that severely affects the respiratory tract, kidneys, and oviducts of poultry (Abaidullah et al., 2021). With the emergence of new IBV variant strains and the lack of cross-protective immunity between different IBV serotypes (Bande et al., 2015; Feng et al., 2015), immune failure is a frequent occurrence. In China, IBV strains can be classified into at least seven genotypes: QX, TW, 4/91, Mass, HN08, LDT3, and Tc07-2, and QX genotype is still the dominant epidemic strain in China (Lee et al., 2021; Zhang et al., 2022).

In this study, we selected RIP for further investigation on the basis of the clinical observations and lesion scores. It was demonstrated that at 3 and 5 dpi, the RIP + zy group had a significantly lower viral load compared to the zy group. A high correlation between viral load and the MLS value was observed. The main pathological changes seen include the detachment of renal tubular epithelial cells, vacuolar degeneration, vasodilatation, and congestion in the zy group. Conversely, in the RIP + zy group, the main pathological changes, including glomerular epithelial cell degeneration, necrosis and lymphocytic infiltration were reduced. Studies have shown that the ameliorative effect of RIP on IBV-induced tissue damage is consistent with the anti-IBV

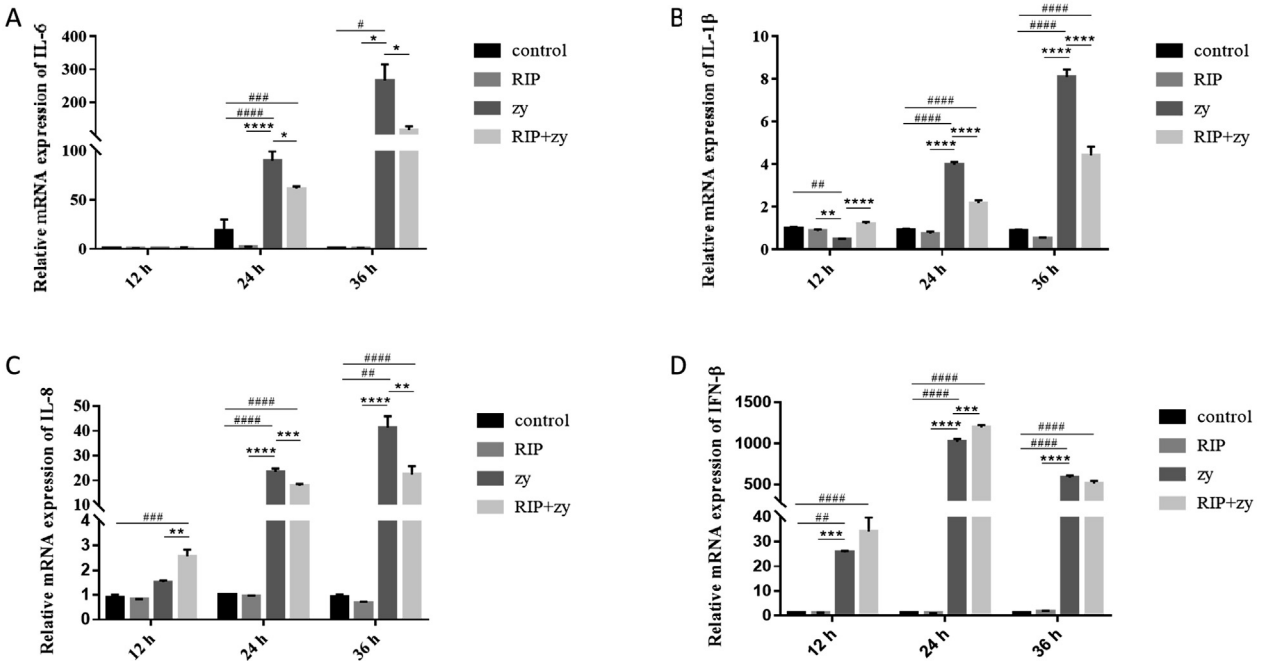

Figure 9. Effects of RIP on cytokine levels in CEK cells treated with zy. Relative mRNA expression levels of (A) IL-6, (B) IL-1β, (C) IL-8, and (D) IFN-β. Data are expressed as the means ± SD, n = 5; $^{\#}P < 0.05$, $^{\#\#}P < 0.01$, $^{\#\#\#}P < 0.001$, $^{\#\#\#\#}P < 0.0001$, compared to the control group; $^{*}P < 0.05$, $^{**}P < 0.01$, $^{***}P < 0.001$, $^{****}P < 0.0001$, compared to the zy group.

effect of other herbal extracts (Zhang et al., 2017; Chen et al., 2019a; b; Wang et al., 2021).

Cytokines play an important role in disease prevention and treatment, particularly in infection, inflammation, and cancer (Guo et al., 2012; Li et al., 2017; Fan et al., 2019; Meng et al., 2019). Inflammatory factors are significantly elevated in IBV-infected cells, promoting tissue lesion and inducing apoptosis. Therefore, inflammatory factors play an important role in inhibition of IBV infections (Zhang et al., 2021). The SARS-CoV infection is known to increase the expressions of inflammatory factors, including IL-1, IL-6, and IL-8, and IBV is similar (Dos Santos et al., 2022). Studies have shown that IBV infection is followed by a significant upregulation of the body's inflammatory factors, including IL-1, IL-6, IL-1β, TNF-α, and MIP-1β (Xiao et al., 2008; Liao et al., 2011; Dar et al., 2014; Zhu et al., 2021; Tang et al., 2022). The results of our study show the same trend and are thus consistent with previous studies. NF-κB can inhibit the production of antiviral interferon and promote the secretion of inflammatory factors that lead to epithelial tissue damage following coronavirus infection (Abaidullah et al., 2021). Some medicines can suppress inflammatory factor expressions by inhibiting the NF-κB signaling pathway. For instance, Licl has been shown to suppress the inflammatory response induced by IBV by downregulating the inflammation-related genes NF-κB, NLRP3, TNF-α, and IL-1β (Liu et al., 2022). The Chinese medicines *Astragalus polysaccharide, forsythoside A, chlorogenic*

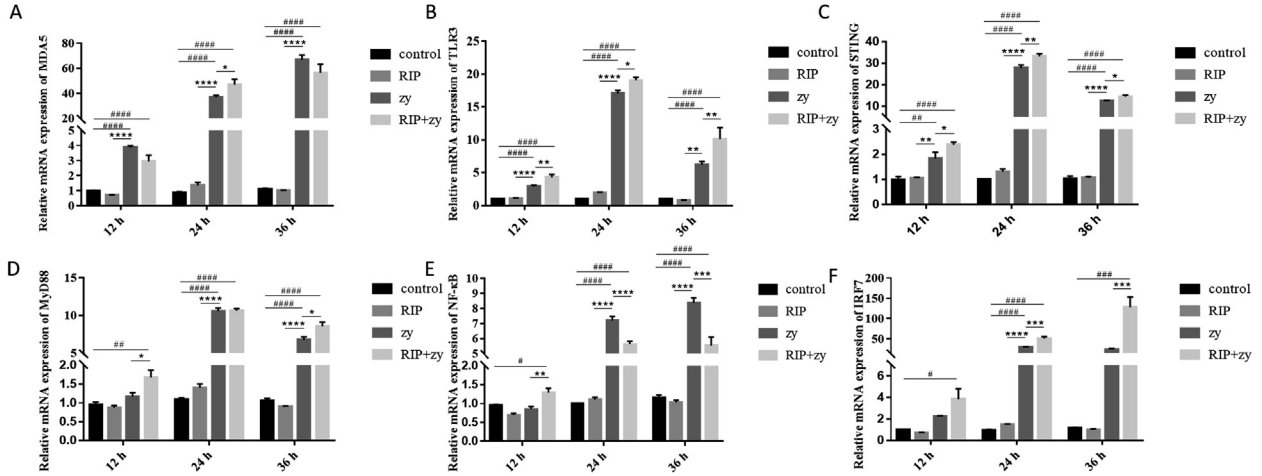

Figure 10. Effects of IPR on MDA5/TLR3 and downstream signal pathways in CEK cells cultures treated with zy. Relative mRNA expression levels of (A) MDA5, (B) TLR3, (C) STING, (D) Myd88, (E) NF-κB, and (F) IRF7. Data are expressed as the means ± SD, n = 5; $^{\#}P < 0.05$, $^{\#\#}P < 0.01$, $^{\#\#\#}P < 0.001$, $^{\#\#\#\#}P < 0.0001$, compared to the control group; $^{*}P < 0.05$, $^{**}P < 0.01$, $^{***}P < 0.001$, $^{****}P < 0.0001$, compared to the zy group.

acid, Shegandilong Granule, and *Doxycycline* was found to modulate the inflammatory response induced by IBV by suppressing NF-κB expression and thus the expression levels of inflammatory factors (Li et al., 2011; Zhang et al., 2017; Abaidullah et al., 2021; Feng et al., 2021). The present study showed that RIP could reduce the expression levels of the inflammatory factors IL-6, IL-8, and IL-1β by decreasing the expression levels of NF-κB, similar to previous studies (Li et al., 2011; Feng et al., 2021).

Regarding the antiviral mechanisms of RIP, we postulated that the anti-IBV effect of RIP may be related to the TLR3, TLR7, and MDA5 signaling pathways, since TLRs, MDA5, and adapter molecules are involved in the recognition of IBV RNA (Xu et al., 2015; Jahan et al., 2020; He et al., 2022). MDA5 consists of two N-terminal cysteine/aspartate protease (caspase) and activation recruitment domain (**CARD**) structural domains (Dias Junior et al., 2019; Jahan et al., 2020). Upon sensing double-stranded RNA, a conformational change occurs, oligomerizing and exposing the N-terminal CARD structural domain and interacting with the CARD structural domain of the signal adaptor, mitochondrial antiviral signaling protein MAVS (Yu et al., 2017). MAVS then signals downstream to activate the IκB-associated kinases, TBK1, and IKKε (Kowalinski et al., 2011), which phosphorylate and induce IRF7 and NF-κB translocation, leading to the production of interferons (**IFN**s) and inflammatory factors (Belgnaoui et al., 2011; Zhou et al., 2020). STING, a molecule downstream of MDA5, is a central adaptor molecule that links the DNA and RNA-sensing pathway and activates IFN-β production, and interacts with MAVS and forms a stable complex in response to viral infection (Ishikawa and Barber, 2008; Nazmi et al., 2012). Other traditional Chinese medicines have also been shown to exert their antiviral effects through similar mechanisms. *Hypericum perforatum L.* was shown to affect IBV replication by upregulating MDA5, MAVS, IFN-α, IFN-β, and downregulating NF-κB, IL-6, and TNF-α in CEK cells, the trachea, and the kidney (Chen et al., 2019). *Chlorogenic acid* affects IBV replication by upregulating MDA5, MAVS, TLR7, MyD88, IRF7, IFN-α, and IFN-β in the trachea and lung (Abaidullah et al., 2021). *Myricetin* exerts antiviral effects on IBV by enhancing ubiquitin modifications of TRAF3 and TRAF6, which PLpro inhibits, and upregulating the activation of the IRF7 signaling pathway (Peng et al., 2022). The present study shows that RIP increased the downstream expression of IFN-β via increasing the MDA5, TLR3, STING, MyD88, and IRF7 signaling pathways in the kidney and CEK cells to resist viral infection, similar to the results of previous studies.

RIP inhibits the production of inflammatory factors by suppressing the NF-κB signaling pathway and activating the MDA5 and TLR3 signal pathways to fight the virus. This suggests a correlation between the ability of RIP to modulate inflammatory factors and the innate immune pathways in RIP-treated and zy-infected kidneys. Therefore, we used principal component analysis to analyze the correlation between the inflammatory factors and the genes related to the immune pathways that are modulated by RIP (Chen et al., 2017; Li et al., 2017; Tan et al., 2017; Xing et al., 2018). The results show that principal component 1 had a large positive correlation with IL-8, MDA5, TLR3, STING, Myd88, and IRF7, suggesting that component 1 may represent components associated with the body's resistance to viral invasion. In contrast, components 2 and 3 showed a greater correlation with IL-6 and IL-8, and it is possible that these components are more relevant to inflammation. Based on the three principal component inflammatory factor scores, the RIP and zy groups had a greater effect on principal component 1, and the scores of the control, RIP + zy, and RIP groups were similar, while the differences between the zy group and the other three groups were greater, indicating that the effect of zy on the three principal components differed significantly from the other 3 groups. According to the three main components of antiviral natural immune pathway genes, the effect of zy + RIP on principle component 1 was greater and positively correlated, suggesting that RIP is responsible for increasing the expressions of genes associated with innate immune pathways, enhancing resistance to viral invasions. Scores of the control, RIP + zy, and RIP groups differed more from the zy group in the three main components, proving that the effect of zy on these three main components was very different from the other three groups. This indicates that RIP treatment can attenuate zy-induced inflammatory kidney injury and zy viral invasion in chickens.

CONCLUSION

In conclusion, this study demonstrates that the anti-IBV properties of RIP may be linked to an inhibition of proinflammatory cytokines, including IL-1β, IL-6, and IL-8 via the NF-κB signaling pathway, and to an upregulation of IFN-β levels via the TLR3 and MDA5 signaling pathways. RIP alleviates kidney enlargement and kidney cell tissue damage while reducing viral load. Further studies are required to elucidate the additional molecular mechanisms to gain a deeper insight into the anti-IBV properties of RIP.

ACKNOWLEDGMENTS

Date Availability Statement: The datasets generated for this study are available on request to the corresponding author.

Author Contributions: YH contributed to the hypothesis generation. JL, MD, NL, LL, and AW contributed to the experimental design, data interpretation, and manuscript preparation. XX conducted the experiments. JX, MC, XH, JX, YS, and SL contributed to the data interpretation.

Funding: This work was financially supported by the Program for Chang-jiang Scholars and Innovative

Research Team in University "PCSIRT" (Grant No. IRTO848).

Ethics Statement: All animal experiments were conducted in compliance with protocols approved by Sichuan Provincial Laboratory Animal Management Committee (Permit Number: SYXK (Sichuan) 2019-187). The protocols for this experiment were performed according to the guidelines of the Ethics and Animal Welfare Committee (EAWC) of the Sichuan Agricultural University.

DISCLOSURES

We declare that we have no financial and personal relationships with other people or organizations that can inappropriately influence our work, there is no professional or other personal interest of any nature or kind in any product, service and/or company that could be construed as influencing the position presented in, or the review of, the manuscript entitled Radix Isatidis polysaccharide (RIP) resists the infection of QX-type Infectious Bronchitis Virus via the MDA5/TLR3/IRF7 signaling pathway

REFERENCES

Abaidullah, M., S. Peng, X. Song, Y. Zou, L. Li, R. Jia, and Z. Yin. 2021. Chlorogenic acid is a positive regulator of MDA5, TLR7 and NF-κB signaling pathways mediated antiviral responses against Gammacoronavirus infection. Int. Immunopharmacol. 96:107671.

Al-Rasheed, M., C. Ball, B. Manswr, G. Leeming, and K. Ganapathy. 2022. Infectious bronchitis virus infection in chicken: viral load and immune responses in Harderian gland, choanal cleft and turbinate tissues compared to trachea. Br. Poult. 63:483–494.

Bande, F., S. S. Arshad, M. H. Bejo, H. Moeini, and A. R. Omar. 2015. Progress and challenges toward the development of vaccines against avian infectious bronchitis. J. Immunol. Res. 2015:424860.

Belgnaoui, S. M., S. Paz, and J. Hiscott. 2011. Orchestrating the interferon antiviral response through the mitochondrial antiviral signaling (MAVS) adapter. Curr. Opin. Immunol. 23:564–572.

Chen, H., I. Muhammad, Y. Zhang, Y. Ren, R. Zhang, X. Huang, L. Diao, H. Liu, X. Li, X. Sun, G. Abbas, and G. Li. 2019. Hypericum perforatum antiviral activity against infectious bronchitis virus and bioactive components of L. Front. Pharmacol. 10:1272.

Chen, J., T. Pan, N. Wan, Z. Sun, Z. Zhang, and S. Li. 2017. Cadmium-induced endoplasmic reticulum stress in chicken neutrophils is alleviated by selenium. J. Inorg. Biochem. 170:169–177.

Dar, A., S. Tikoo, A. Potter, L. A. Babiuk, H. Townsend, V. Gerdts, and G. Mutwiri. 2014. CpG-ODNs induced changes in cytokine/chemokines genes expression associated with suppression of infectious bronchitis virus replication in chicken lungs. Vet. Immunol. Immunopathol. 160:209–217.

Dias Junior, A. G., N. G. Sampaio, and J. Rehwinkel. 2019. A balancing act: MDA5 in antiviral immunity and autoinflammation. Trends Microbiol. 27:75–85.

Dos Santos, A., L. E. Rodrigues, A. L. Alecrim-Zeza, L. de Araújo Ferreira, C. Trettel, G. M. Gimenes, A. F. Da Silva, C. Sousa-Filho, T. Serdan, A. C. Levada-Pires, E. Hatanaka, F. T. Borges, M. P. de Barros, M. F. Cury-Boaventura, G. L. Bertolini, P. Cassolla, G. N. Marzuca-Nassr, K. F. Vitzel, T. C. Pithon-Curi, L. N. Masi, R. Curi, R. Gorjao, and S. M. Hirabara. 2022. Molecular and cellular mechanisms involved in tissue-specific metabolic modulation by SARS-CoV-2. Front. Microbiol. 13:1037467.

Du, Z., H. Liu, Z. Zhang, and P. Li. 2013. Antioxidant and anti-inflammatory activities of Radix Isatidis polysaccharide in murine alveolar macrophages. Int. J. Biol. Macromol. 58:329–335.

Echeverría-Bugueño, M., C. Balada, R. Irgang, and R. Avendaño-Herrera. 2021. Evidence for the existence of extracellular vesicles in Renibacterium salmoninarum and related cytotoxic effects on SHK-1 cells. J. Fish Dis. 44:1015–1024.

Fan, S., J. Li, and B. Bai. 2019. Purification, structural elucidation and in vivo immunity-enhancing activity of polysaccharides from quinoa (Chenopodium quinoa Willd.) seeds. Biosci. Biotechnol. Biochem. 83:2334–2344.

Feng, H., X. Wang, J. Zhang, K. Zhang, W. Zou, K. Zhang, L. Wang, Z. Guo, Z. Qiu, G. Wang, R. Xin, and J. Li. 2021. Combined effect of shegandilong granule and doxycycline on immune responses and protection against avian infectious bronchitis virus in broilers. Front. Vet. Sci. 8:756629.

Feng, K., Y. Xue, J. Wang, W. Chen, F. Chen, Y. Bi, and Q. Xie. 2015. Development and efficacy of a novel live-attenuated QX-like nephropathogenic infectious bronchitis virus vaccine in China. Vaccine 33:1113–1120.

Gallardo, R. A., A. P. Da Silva, R. Gilbert, M. Alfonso, A. Conley, K. Jones, P. A. Stayer, and F. J. Hoerr. 2022. Testicular atrophy and epididymitis-orchitis associated with infectious bronchitis virus in broiler breeder roosters. Avian. Dis. 66:112–118.

Ganapathy, K. 2021. Infectious bronchitis virus infection of chicken: the essential role of mucosal immunity. Avian. Dis. 65:619–623.

Guo, L., J. Liu, Y. Hu, D. Wang, Z. Li, J. Zhang, T. Qin, X. Liu, C. Liu, X. Zhao, Y. P. Fan, G. Han, and T. L. Nguyen. 2012. Astragalus polysaccharide and sulfated epimedium polysaccharide synergistically resist the immunosuppression. Carbohyd. Polym. 90:1055–1060.

He, T., M. Wang, A. Cheng, Q. Yang, Y. Wu, R. Jia, S. Chen, D. Zhu, M. Liu, X. Zhao, S. Zhang, J. Huang, B. Tian, X. Ou, S. Mao, D. Sun, Q. Gao, Y. Yu, L. Zhang, and Y. Liu. 2022. Duck plague virus UL41 protein inhibits RIG-I/MDA5-mediated duck IFN-β production via mRNA degradation activity. Vet. Res. 53:22.

Ishikawa, H., and G. N. Barber. 2008. STING is an endoplasmic reticulum adaptor that facilitates innate immune signalling. Nature 455:674–678.

Jahan, A. S., E. Biquand, R. Muñoz-Moreno, A. Le Quang, C. K. Mok, H. H. Wong, Q. W. Teo, S. A. Valkenburg, A. Chin, L. L. Man Poon, A. Te Velthuis, A. García-Sastre, C. Demeret, and S. Sanyal. 2020. OTUB1 is a key regulator of RIG-I-dependent immune signaling and is targeted for proteasomal degradation by influenza a NS1. Cell Rep. 30:1570–1584.

Kong, L., R. You, D. Zhang, Q. Yuan, B. Xiang, J. Liang, Q. Lin, C. Ding, M. Liao, L. Chen, and T. Ren. 2021. Infectious bronchitis virus infection increases pathogenicity of H9N2 avian influenza virus by inducing severe inflammatory response. Front. Vet. Sci. 8:824179.

Kowalinski, E., T. Lunardi, A. A. McCarthy, J. Louber, J. Brunel, B. Grigorov, D. Gerlier, and S. Cusack. 2011. Structural basis for the activation of innate immune pattern-recognition receptor RIG-I by viral RNA. Cell 147:423–435.

Lee, H. C., S. Jeong, A. Y. Cho, K. J. Kim, J. Y. Kim, D. H. Park, H. J. Kim, J. H. Kwon, and C. S. Song. 2021. Genomic analysis of avian infectious bronchitis viruses recently isolated in South Korea reveals multiple introductions of GI-19 lineage (QX Genotype). Viruses 13:1045.

Li, H., J. Wu, Z. Zhang, Y. Ma, F. Liao, Y. Zhang, and G. Wu. 2011. Forsythoside a inhibits the avian infectious bronchitis virus in cell culture. Phytother. Res. 25:338–342.

Li, J., Y. Liu, J. Fang, X. Chen, and W. Xie. 2007. Effect of Radix Isatidis on the expression of moesin mRNA induced by LPS in the tissues of mice. J. Huazhong Univ. Sci. Technol. Med. Sci. 27:135–137.

Li, S., S. Fan, N. Li, Y. Shen, X. Xiang, W. Chen, J. Xia, X. Han, M. Cui, and Y. Huang. 2022. The N1038S substitution and EQTRPKKSV deletion of the S2 subunit of QX-type avian infectious bronchitis virus can synergistically enhance viral proliferation. Front. Microbiol. 13:829218.

Li, X., M. Xing, M. Chen, J. Zhao, R. Fan, X. Zhao, C. Cao, J. Yang, Z. Zhang, and S. Xu. 2017. Effects of selenium-lead interaction on the gene expression of inflammatory factors and selenoproteins in chicken neutrophils. Ecotox. Environ. Safe 139:447–453.

Liao, Y., X. Wang, M. Huang, J. P. Tam, and D. X. Liu. 2011. Regulation of the p38 mitogen-activated protein kinase and dual-specificity phosphatase 1 feedback loop modulates the induction of interleukin 6 and 8 in cells infected with coronavirus infectious bronchitis virus. Virology 420:106–116.

Liu, X., X. Chang, Q. Wu, J. Xu, L. Chen, R. Shen, and X. Hou. 2022. Lithium chloride inhibits infectious bronchitis virus-induced apoptosis and inflammation. Microb. Pathog. 162:105352.

Liu, Y., M. Chen, Q. Guo, Y. Li, J. Jiang, and J. Shi. 2017. Aromatic compounds from an aqueous extract of "ban lan gen" and their antiviral activities. Acta Pharm. Sinica. B 7:179–184.

Meng, M., M. Guo, C. Feng, R. Wang, D. Cheng, and C. Wang. 2019. Water-soluble polysaccharides from Grifola Frondosa fruiting bodies protect against immunosuppression in cyclophosphamide-induced mice via JAK2/STAT3/SOCS signal transduction pathways. Food Funct. 10:4998–5007.

Nazmi, A., R. Mukhopadhyay, K. Dutta, and A. Basu. 2012. STING mediates neuronal innate immune response following Japanese encephalitis virus infection. Sci. Rep.-Uk 2:347.

Ni, L. J., L. G. Zhang, J. Hou, W. Z. Shi, and M. L. Guo. 2009. A strategy for evaluating antipyretic efficacy of Chinese herbal medicines based on UV spectra fingerprints. J Ethnopharmacol. 124:79–86.

Peng, S., C. Fang, H. He, X. Song, X. Zhao, Y. Zou, L. Li, R. Jia, and Z. Yin. 2022. Myricetin exerts its antiviral activity against infectious bronchitis virus by inhibiting the deubiquitinating activity of papain-like protease. Poult. Sci. 101:101626.

Shin, E. K., D. H. Kim, H. Lim, H. K. Shin, and J. K. Kim. 2010. The anti-inflammatory effects of a methanolic extract from Radix Isatidis in murine macrophages and mice. Inflammation 33:110–118.

Tan, S., Q. Chi, T. Liu, Z. Sun, Y. Min, Z. Zhang, and S. Li. 2017. Alleviation mechanisms of selenium on cadmium-spiked neutrophil injury to chicken. Biol. Trace Elem. Res. 178:301–309.

Tang, X., J. Qi, L. Sun, J. Zhao, G. Zhang, and Y. Zhao. 2022. Pathological effect of different avian infectious bronchitis virus strains on the bursa of Fabricius of chickens. Avian Pathol 51:1–31.

Wang, X., X. Li, X. Wang, L. Chen, E. Ning, Y. Fan, H. Wang, T. Chen, and W. Wang. 2021. Experimental study of forsythoside A on prevention and treatment of avian infectious bronchitis. Res. Vet. Sci. 135:523–531.

Xia, J., X. He, L. J. Du, Y. Y. Liu, G. J. You, S. Y. Li, P. Liu, S. J. Cao, X. F. Han, and Y. Huang. 2018. Preparation and protective efficacy of a chicken embryo kidney cell-attenuation GI-19/QX-like avian infectious bronchitis virus vaccine. Vaccine 36:4087–4094.

Xiao, H., L. H. Xu, Y. Yamada, and D. X. Liu. 2008. Coronavirus spike protein inhibits host cell translation by interaction with eIF3f. Plos One 3:e1494.

Xing, M., X. Jin, J. Wang, Q. Shi, J. Cai, and S. Xu. 2018. The antagonistic effect of selenium on lead-induced immune dysfunction via recovery of cytokine and heat shock protein expression in chicken neutrophils. Biol. Trace Elem. Res. 185:162–169.

Xu, Y., T. Zhang, Q. Xu, Z. Han, S. Liang, Y. Shao, D. Ma, and S. Liu. 2015. Differential modulation of avian β-defensin and Toll-like receptor expression in chickens infected with infectious bronchitis virus. Appl. Microbiol. Biot. 99:9011–9024.

Yu, L., X. Zhang, T. Wu, J. Su, Y. Wang, Y. Wang, B. Ruan, X. Niu, and Y. Wu. 2017. Avian infectious bronchitis virus disrupts the melanoma differentiation associated gene 5 (MDA5) signaling pathway by cleavage of the adaptor protein MAVS. Bmc. Vet. Res. 13:332.

Zamzam, S. H., A. Ghalyanchilangeroudi, and A. R. Khosravi. 2022. Comparative trachea transcriptome analysis in SPF broiler chickens infected with avian infectious bronchitis and avian influenza viruses. Virus Genes 58:203–213.

Zhang, P., J. Wang, W. Wang, X. Liu, H. Liu, X. Li, and X. Wu. 2017. Astragalus polysaccharides enhance the immune response to avian infectious bronchitis virus vaccination in chickens. Microb. Pathog. 111:81–85.

Zhang, X., K. Yan, C. Zhang, M. Guo, S. Chen, K. Liao, Z. Bo, Y. Cao, and Y. Wu. 2022. Pathogenicity comparison between QX-type and Mass-type infectious bronchitis virus to different segments of the oviducts in laying phase. Virol. J. 19:62.

Zhang, Y., Z. Xu, and Y. Cao. 2021. Host antiviral responses against avian infectious bronchitis virus (IBV): focus on innate immunity. Viruses 13:1698.

Zhao, Y. L., J. B. Wang, L. M. Shan, C. Jin, L. Ma, and X. H. Xiao. 2008. Effect of Radix isatidis polysaccharides on immunological function and expression of immune related cytokines in mice. Chin. J. Integr. Med. 14:207–211.

Zhou, R., Q. Zhang, and P. Xu. 2020. TBK1, a central kinase in innate immune sensing of nucleic acids and beyond. Acta Bioch. Bioph. Sin. 52:757–767.

Zhou, W., and X. Y. Zhang. 2013. Research progress of Chinese herbal medicine Radix isatidis (banlangen). Am. J. Chinese Med. 41:743–764.

Zhu, Q. C., S. Li, L. X. Yuan, R. A. Chen, D. X. Liu, and T. S. Fung. 2021. Induction of the proinflammatory chemokine interleukin-8 is regulated by integrated stress response and AP-1 family proteins activated during coronavirus infection. Int. J. Mol. Sci. 22:5646.